Journal of Machine Engineering, Vol. 17, No. 4, 54-68, 2017
ISSN 1895-7595 (Print) ISSN 2391-8071 (Online)

Received: *11 September 2017* / Accepted: *10 October 2017* / Published online: *20 October 2017*

surface roughness, quickpoint grinding, Cubitron™ II grinding wheels,

Czeslaw NIZANKOWSKI[1]
Grzegorz STRUZIKIEWICZ[1*]
Andrzej MATRAS[1]

SIMULATION ROUGHNESS OF THE STEEL ROLLERS' SURFACE LAYER WITH CUBITRON™ II GRINDING WHEELS BY THE QUICKPOINT TECHNIQUE

This paper describes a simulation model of the process of developing steel rollers' surface layer roughness obtained with Cubitron™ II grinding wheels by the Quickpoint technique, depending on the assumed grinding conditions. In particular, the authors present physical assumptions of the respective model, a conception and algorithm of its operation, and the results of simulation tests. The results were later verified in specific experiments by comparing the statistical average values of the selected ground steel rollers' surface roughness parameters with the values generated by simulations.

1. INTRODUCTION

Poland belongs to a small group of the countries producing a series of small-calibre (up to 30 mm) guns and artillery and missile weapon systems.

Owing to the high fire-rate and consequential dynamic mechanical and thermal loads, the barrels of such systems have to be made of proper high-alloy steel, with improved mechanical properties. The barrels are designed for easy periodic replacement, with the use of a special latch and barrel-bolt system. The profiles and surface roughness of those barrel components are obtained in two process passes.

The authors of this paper decided to check the possibility of producing the said structural elements of the barrel in one pass only, using the so-called Quickpoint technique [1,2]. The essence of that modern grinding technique, patented by the Junker GmbH, consists in a single-pass removal of the workpiece material along the complex workpiece profile, with observation of the low components of grinding force, low effective grinding power, and point-sized contact between the grinding wheel and the surface being processed, as well as with continuous grinding-wheel path control (CPCG – Continuous Path Controlled Grinding).

[1] Production Engineering Institute of the Mechanical Faculty, Cracow University of Technology, Cracow, Poland
[*] E-mail: struzikiewicz@mech.pk.edu.pl
DOI: 10.5604/01.3001.0010.7005

The point contact between the grinding wheel active surface (GWAS) and the ground roller's surface is obtain in the Quickpoint technique by twisting the grinding wheel axis in respect of the roller axis by the angle from 0.5° to the maximum of about a dozen degrees, depending on the grinding wheel's characteristics, workpiece material properties, and grinder's operating capabilities. Consequently, the roller surface and GWAS are intersecting at one point only (Fig. 1).

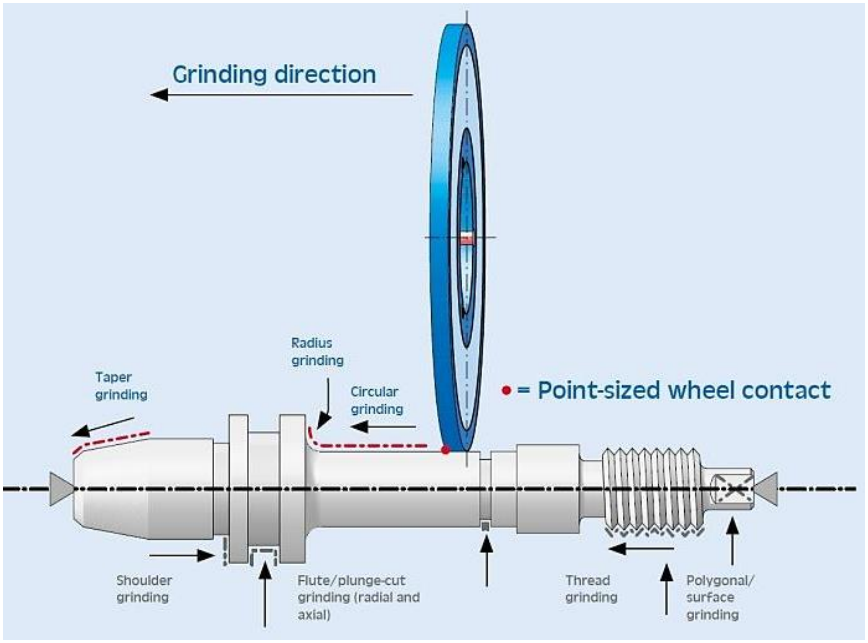

Fig. 1. The essence of rotational body grinding, with the use of the Quickpoint technique [1]

We should emphasise here that the technique in question relies on thin grinding wheels that are 5-7 mm high and mostly made of CBN or PCD superhard abrasives, either electroplated or with sintered metal bonds. The grinding velocities belong to the range from 45 to 90 m/s [3,4]. Such grinding wheels are expensive and they must be structurally suitable for special Junker GmbH grinders (Fig. 2) [1,4,5]. For that reason, the authors decided to use in their tests the grinding wheels made of microcrystalline sintered corundum, sold under the trade name of Cubitron™ II, manufactured by the 3M in the USA.

Fig. 2. Junker Quickpoint grinding machine [1]

The abrasive is mounted in strengthened phenol-formaldehyde resin binder. Such grinding wheels can be used with the grinding velocity of up to 80 m/s (Fig. 3) [4].

Fig. 3. Cubitron™ II grinding wheels [3,4]

The microcrystalline sintered corundum of the Cubitron™ II grinding wheels constitutes a creative and technological development of the Cubitron abrasive that has been manufactured for over thirty years with the use of the sol-gel method. Its particular features include abrasive grains formed by the micro-replication method, shaped as regular prisms, with the equilateral triangle base and low height (Fig. 4).

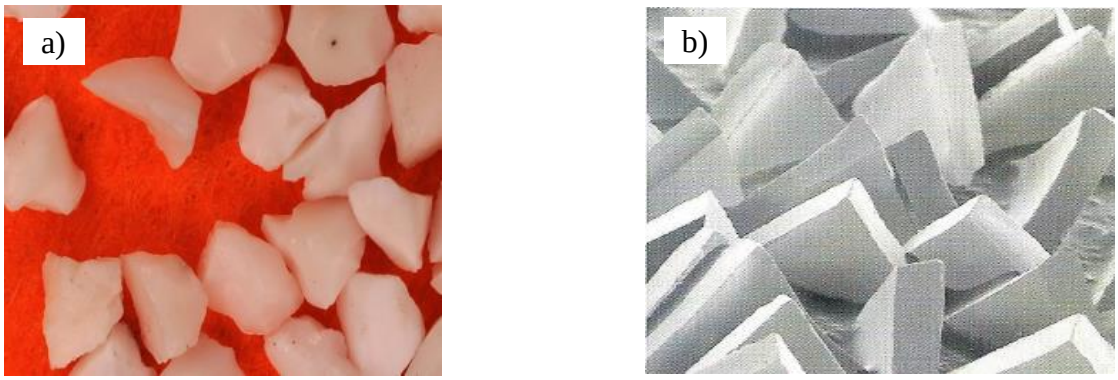

Fig. 4. Abrasive grains of the microcrystalline sintered corundum:
(a) Cubitron™ and (b) Cubitron™ II [4]

Cubitron™ II abrasives are produced in the granulation sizes of 46+, 60+, and 80+. The "+" sign added to the abrasive grain numbers means that the Cubitron™ II grains are larger than the classical abrasive grains. Generally, the Cubitron™ II grinding wheels, in comparison to those of Cubitron™ of the first generation, allow for obtaining higher grinding effectiveness, higher grain durability, lower temperature and grinding power, as well as increased grinding process safety. Currently, Cubitron™ II grinding wheels are manufactured in the following types: 1, 4, 5, 11, 12, and 27, although only the latter are low height. Up till now, the tests involving the processes of obtaining correct properties of the grinded surfaces, with the use of microcrystalline sintered corundum grinding wheels, have been described by about a dozen of authors [6-13]. However, those tests did not involve the Quickpoint technique.

2. SIMULATION MODEL

Taking into account the fact that the assumptions of a simulation model should constitute a compromise between exact reflection of the real conditions and the structure of a possibly simple simulation algorithm [14-17], the authors built a simulation model of the development of steel roller surface roughness, with the following physical assumptions:

- a full characteristics of the Cubitron™ II grinding wheel is known,
- circular grinding of the external roller surfaces is conducted in accordance with the Quickpoint kinematics,
- the values of all the grinding process parameters are known,
- the input profile of the surface layer roughness of the workpiece is known,
- the linear profiles of the Cubitron™ II grinding wheel active surface (GWAS) are known (Fig. 5),
- the angle of grinding wheel twist in respect of the roller axis is known,
- the value of grinding wheel infeed to the workpiece and the value of the roller's elastic deflection is known,
- the workpiece is a body of uniform material properties,
- the phenomenon of pure micro-machining of the workpiece and local elastic deformation occurs exclusively in the grinding process,
- the process of the development of the workpiece's surface layer roughness is represented by each removal of the workpiece's common parts of the workpiece profile and the grinding-wheel active surface, with the use of the image recognition techniques.

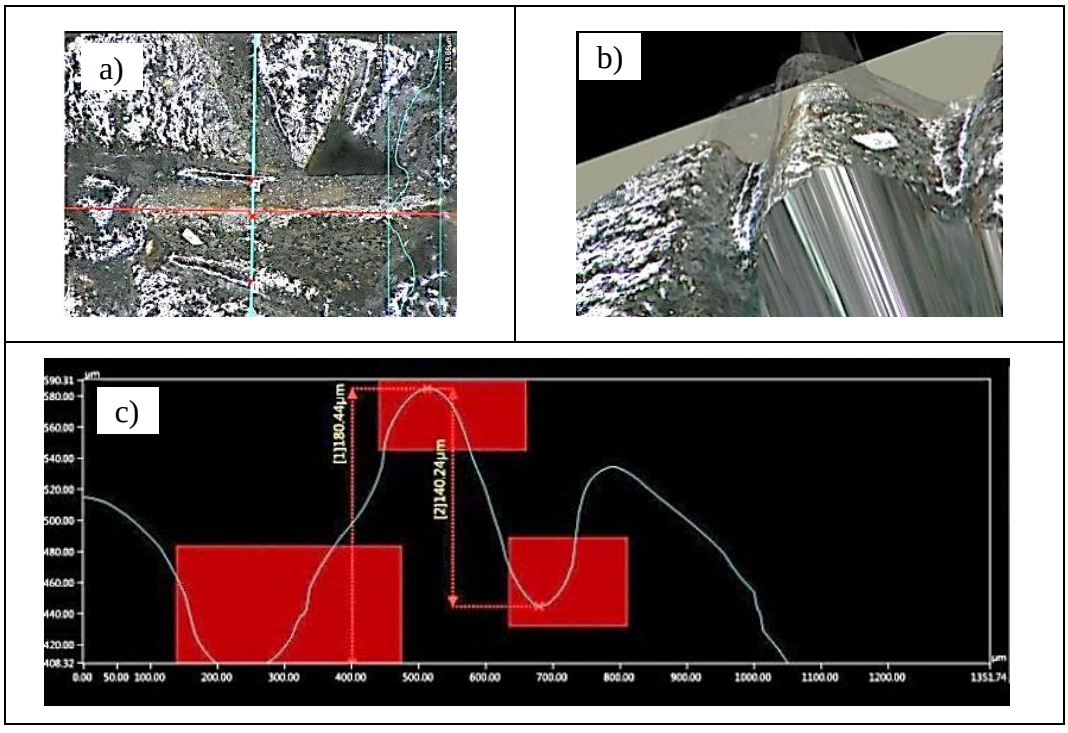

Fig. 5. The technique of the identification of the Cubitron™ II abrasive grain location on the profile of the grinding-wheel surface active (a Keyence microscope)

Our assumption of the lack of the necessity to consider grooving processes of the workpiece's surface layer roughness in the present simulation model, when surface machining is conducted with single abrasive grains of Cubitron™ II, in the conditions of large grinding wheel in feeds (e.g. by 0.2 mm), was based on the specification made by a 3M representative, assuring a considerable domination of the pure micro-machining process.

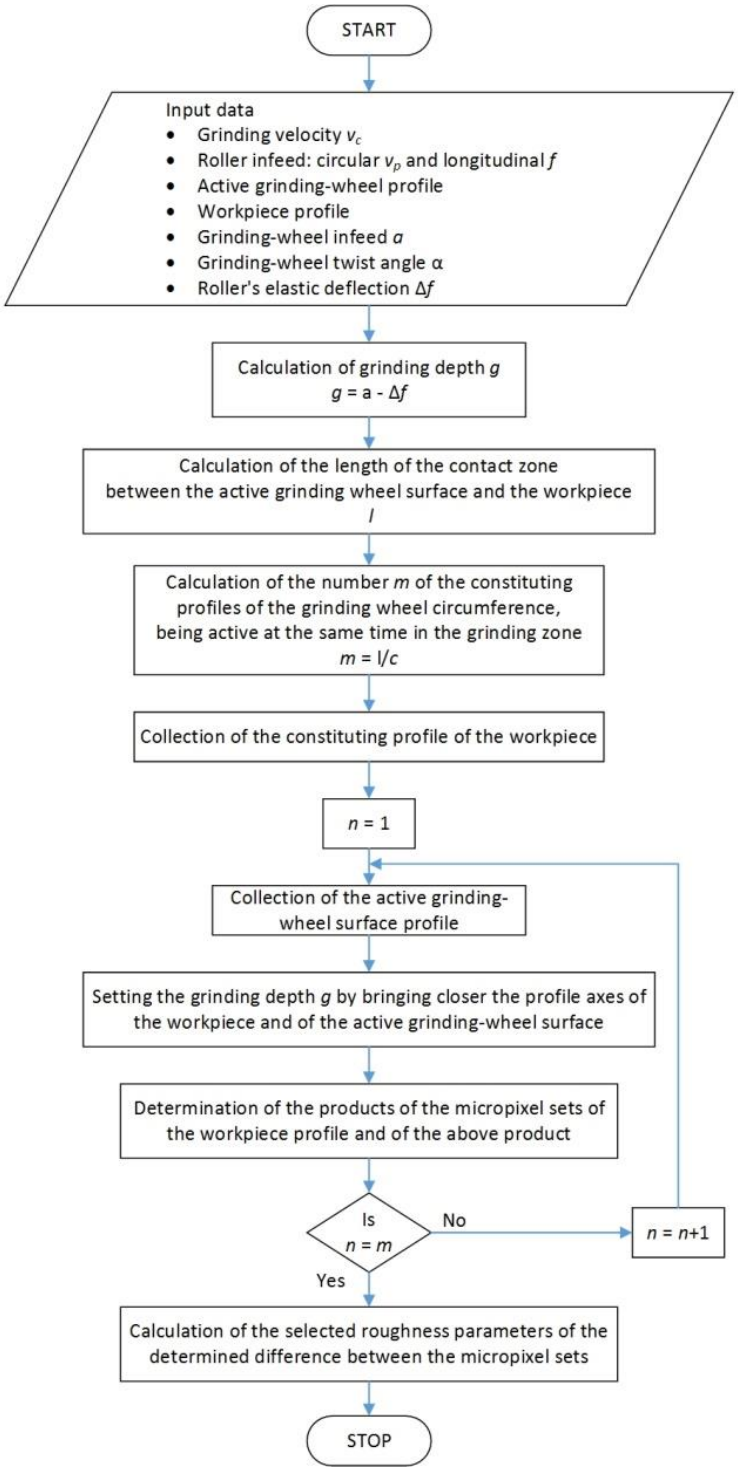

Fig. 6. A block diagram of the simulation model algorithm

Fig. 6 presents a block diagram of the algorithm of the simulation model in question. The algorithm was transformed into the NIZMAT2 simulation software. Fig. 7 illustrates the method of determining the products of the micropixel sets of the workpiece profile and of the grinding-wheel active surface profile. Fig. 8 shows a sample view of grinding-wheel active surface along the constituting surface of the grinding wheel's circumference.

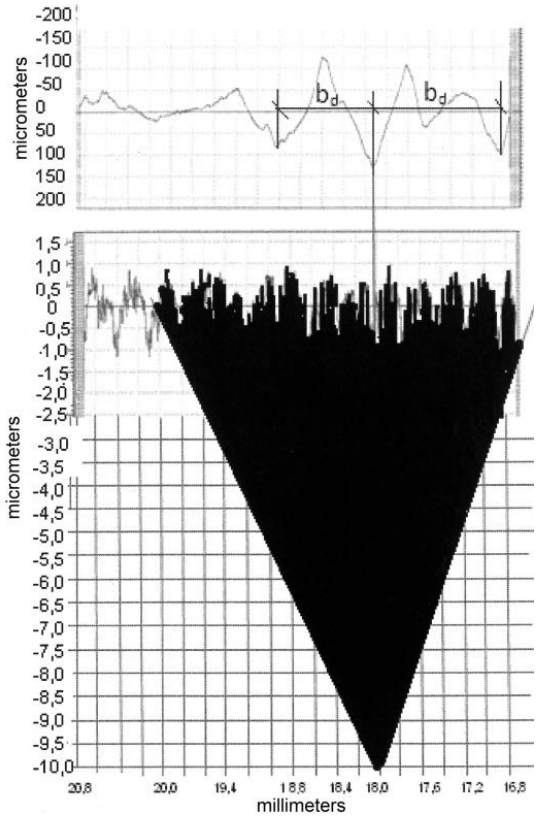

Fig. 7. The conception of determining a new surface layer profile of a workpiece

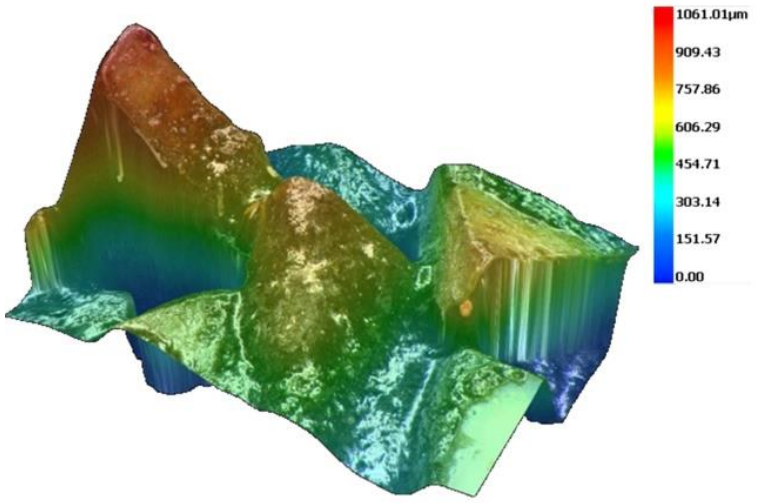

Fig. 8. Allocation of the Cubitron™ II abrasive grains on the grinding-wheel active surface (magnification: 50×)

3. SIMULATION EXPERIMENTS AND EXPERIMENTAL TESTS

The NIZMAT2 simulation software was designed and a test workbench was constructed, with the use of a 3Z42 universal tool grinder, to conduct three simulation tests and three experimental tests in the same grinding conditions by the Quickpoint technique [18].

In both types of the tests, 3M (USA) 65509 27 150x7x22.23 XC90 1060 903 grinding wheels were used. The grinding wheels were made of Cubitron™ II abrasive grains number 60+ on phenol-formaldehyde binder. The average distance between the grains was 1.4 ± 0.21 mm.

Fig. 9 presents the surface layer roughness profile of the grinded roller, with the values of selected profile parameters.

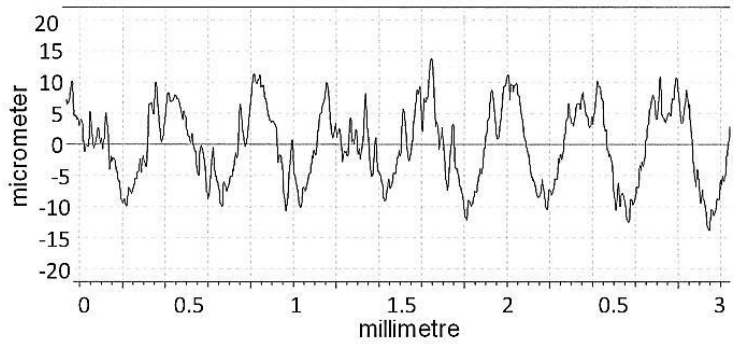

Ra	5.285	Rv	11.709	Rp	11.528

Fig. 9. Constituting workpiece profile roughness

Fig. 10 presents one of the 30 grinding-wheel active surface profiles, with identified grain locations.

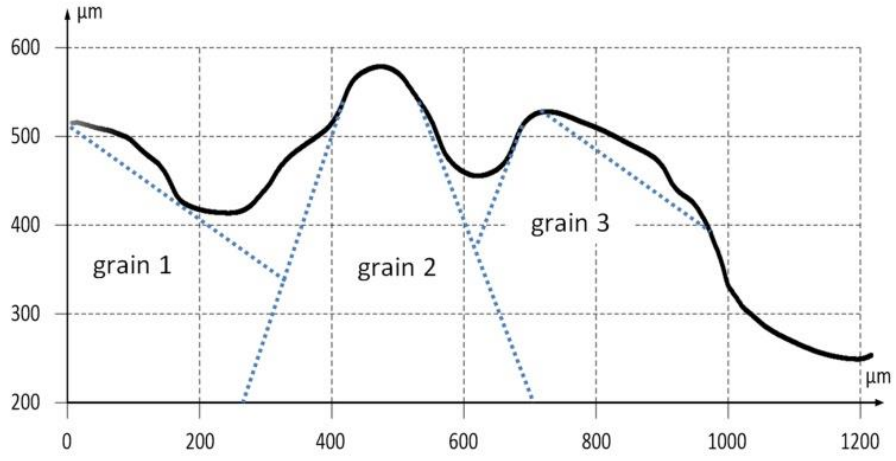

Fig. 10. Sample grinding-wheel active surface profile

The following values of grinding parameters were assumed:

- grinding velocity v_c = 50 m/s,
- infeed of the grinding wheel to the workpiece a = 0.1 mm,
- circumferential infeed of the roller v_p = 5 m/min.,
- longitudinal infeed of the roller f = 0.02 m/min.,
- grinding wheel's twist angle $\alpha = 12°$.

As a result of the completed simulation experiments, grinded surface roughness profiles were obtained. They were characterised by the following values of selected roughness parameters *Rz*, *Rp*, *Rv*, and *RSm* (Table 1).

Table 1. The values of the selected roughness parameters of the grinded roller surface roughness profiles generated by simulation

Parameter	Profile 1	Profile 2	Profile 3	Average Value
Rz (μm)	24	29	25	26.00
Rp (μm)	10	16	12	12.67
Rv (μm)	10	14	14	12.67
RSm (μm)	160	190	183	177.67

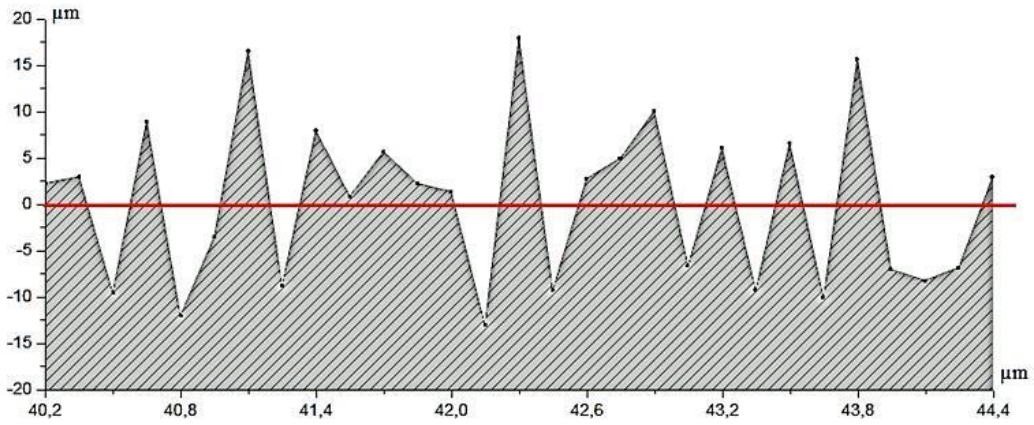

Fig. 11. Sample grinded surface roughness profile generated by simulations (modified profile)

Unfortunately, the NIZMAT2 software cannot calculate the values of other roughness parameters of the grinded surface or determine the material share curve (Abbot curve). Next, using the same grinding parameters and using a grinding wheel which has the identical characteristics as that assumed in the simulation tests, an experimental bench was implemented to test the roller made of alloy structural steel, designed for the production of elements under specific loads (made of classified steel grade). The roughness profile of the roller was taken into account earlier in the simulation tests (Fig. 8).

The general view of the test bench is presented in Fig. 12. Fig. 13 presents the view of the roller grinding zone, using a Cubitron™ II grinding wheel and the Quickpoint technique.

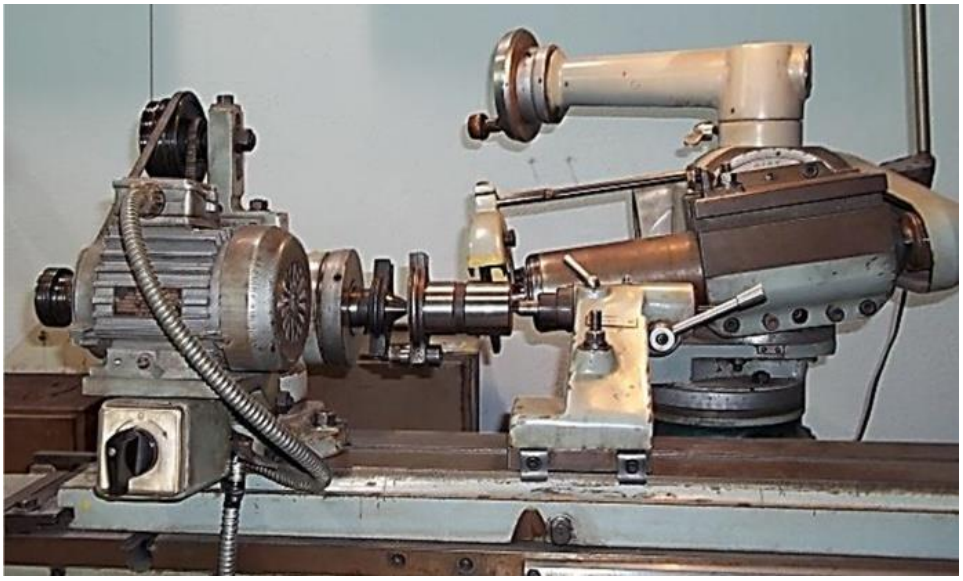

Fig. 12. Test bench for external circumferential grinding, using the Quickpoint technique

Fig. 13. Zone of grinding with a Cubitron™ II grinding wheel

Since no access to a Junker GmbH grinding machine was available, the analysts resigned of special narrow Cubitron™ II grinding wheels, with metal core that can be produced by 3M to order, and used rather Type 27 grinding wheels for angular grinding (Fig. 3).

Such tests were conducted with the application of a Taylor-Hobson Form 50 stylus profilometer (Fig. 14). As a result of the experimental tests, roughness profiles of the grinded surface were obtained, as presented in Fig. 15, characterised by the values of the selected roughness parameters (*Rz*, *Rp*, *Rm*, and *Rsm*), specified in Table 2.

a) b)

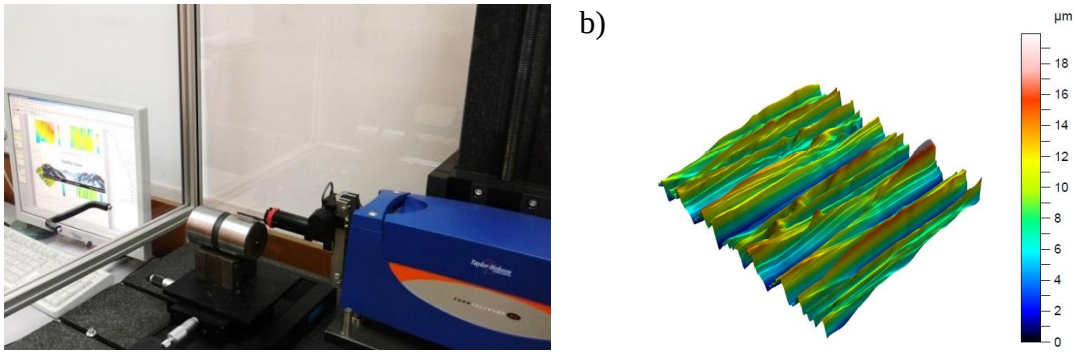

Fig. 14. A general view of the stylus profilometer (a) and the object being measured and geometrical structure of the steel roller's surface in 3D system (b)

Table 2. The values of selected roughness parameters of the grinded roller surface determined in experiments

Parameter	Profile 1	Profile 2	Profile 3	Average Value
Rz (µm)	20.86	26.42	21.04	22.77
Rp (µm)	9.79	14.07	8.68	10.85
Rv (µm)	11.06	12.34	12.36	11.92
RSm (µm)	177.27	173.91	154.66	168.61

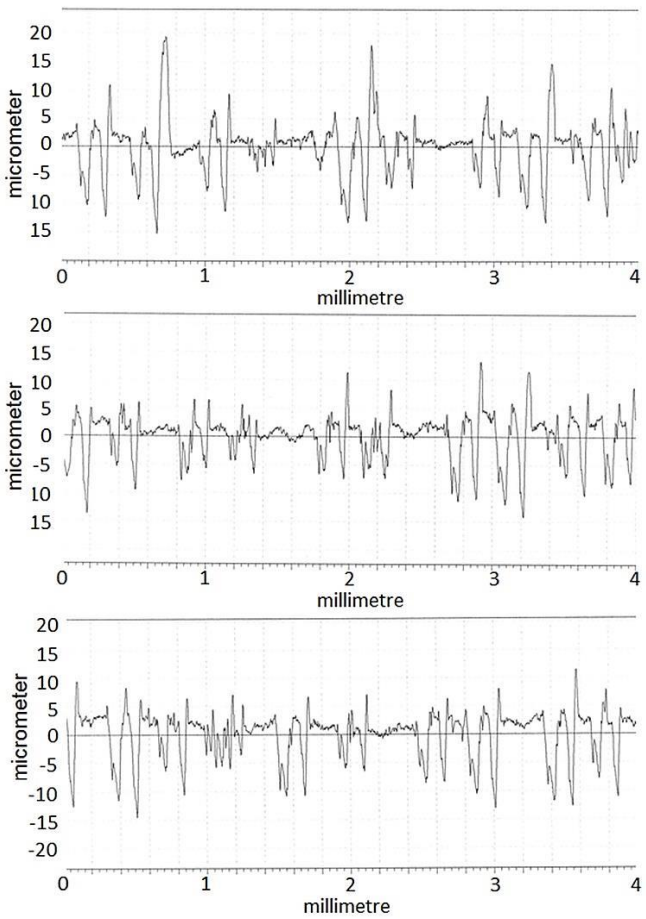

Fig. 15. Roughness profiles of the grinded roller surface measured by experiments (modified profiles)

4. COMPARATIVE ANALYSIS OF THE SIMULATION AND EXPERIMENTAL TEST RESULTS

The results of simulation and experimental tests conducted on an actual object, expressed by the values of selected roughness parameters of the grinded surface, were subjected to a statistical analysis. In the first stage of that analysis, the average values with standard deviations were compared taking into account the same roughness parameters from both groups of test results (Figs. 16 a, b, c, d).

a)

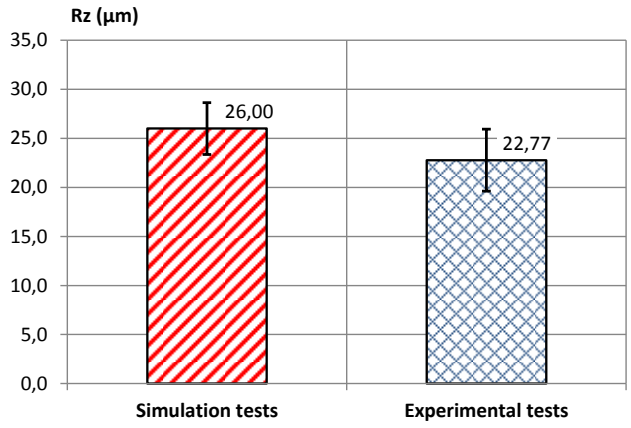

b)

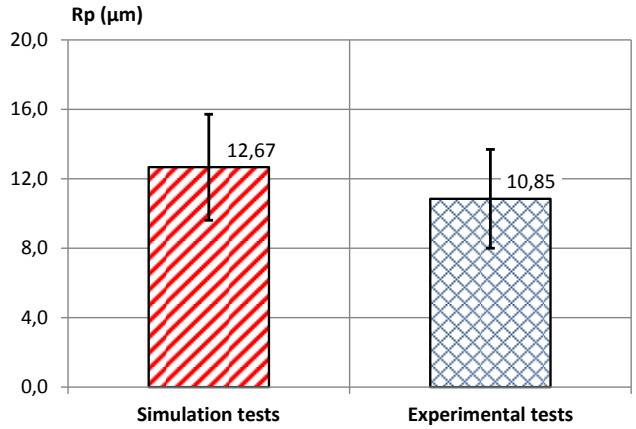

c)

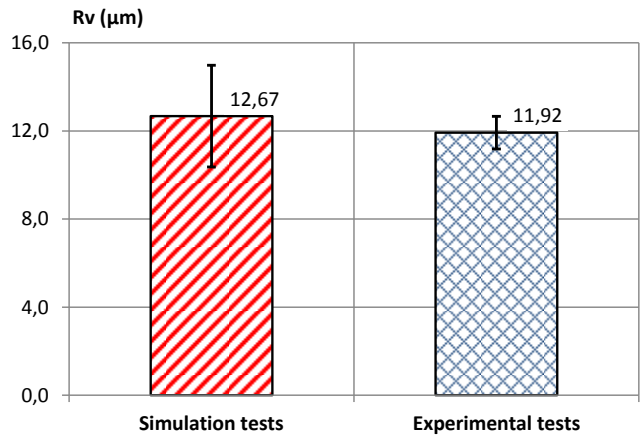

d)

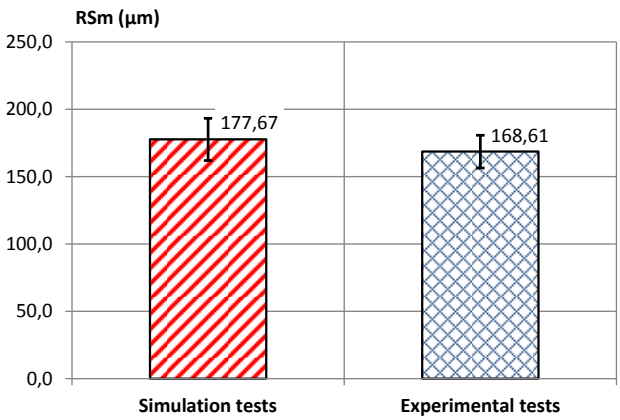

Fig. 16. Histograms of simulation and experimental test results

Next, the authors tried to establish whether the ratio of two variances (of both test result groups), for the same roughness parameter of the grinded surface, is larger than one could expect in the case when the samples are collected from the same population. Therefore, the following zero hypotheses were posed:

$$H_0: \begin{matrix} \sigma^2(Rz') = \sigma^2(Rz") \\ \sigma^2(Rp') = \sigma^2(Rp") \\ \sigma^2(Rv') = \sigma^2(Rv") \\ \sigma^2(RSm') = \sigma^2(RSm") \end{matrix} \Bigg\} \tag{1}$$

To verify those hypotheses, the expressions $s^2(R')$ i $s^2(R")$ were used as estimations of the variances of the altering values of the roughness parameters *Rz*, *Rp*, *Rv*, and *RSm* (on the basis of samples), together with the Fisher-Snedecor statistical distribution:

$$F = \frac{s^2(R")}{s^2(R')} \tag{2}$$

The results of the variance analysis by the *F* test are presented in Table 3.

Table 3. The variance analysis by the *F* test applied to the simulation and experimental test results of the grinded surface roughness by Cubitron™ II grinding wheels

Parameter	Calculated values of *F*	Critical values $F_{critical}$	
		$F_{0.05:2:2}$	$F_{0.1:2:2}$
Rz (µm)	0.70	19.0	99.0
Rp (µm)	1.15		
Rv (µm)	9.61		
RSm (µm)	1.65		

The comparison of the calculated values *F* with the critical values $F_{critical}$ does not allow for the rejection of the zero hypothesis H_0 with the variance equation at the materiality levels of $\alpha = 0.05$ i $\alpha = 0.1$.

$$F<F_{0.05:2:2} \text{ and } F<F_{0.05:2:2} \tag{3}$$

In the second stage of statistical analysis of the test results, the authors checked whether there is a significant difference between two average values of $\overline{R}z, \overline{R}p, \overline{R}v, \overline{R}Sm$ (of both test result groups), for the same roughness parameter of the grinded surface. Therefore, the following zero hypotheses were posed:

$$H_0: \left.\begin{array}{r} \overline{Rz}' = \overline{Rz}" \\ \overline{Rp}' = \overline{Rp}" \\ \overline{Rv}' = \overline{Rv}" \\ \overline{RSm}' = \overline{RSm}" \end{array}\right\} \tag{4}$$

where: $\overline{Rx}'x$, $\overline{Rx}"x$ – two separate arithmetic averages.

When verifying those hypotheses, test *t* was applied to check the difference between the two averages [13].

$$t = \frac{\left|\overline{Rx}'x - \overline{Rx}"x\right|}{\bar{s}(Rx's, Rx"x)\cdot\sqrt{\frac{n_1+n_2}{n_1\cdot n_2}}} \tag{5}$$

where: n_1 and n_2 – the number of samples from which $\overline{Rx}'x$, $\overline{Rx}"x$ were calculated; $\bar{s}(Rx'x, Rx"x)$ – total estimation of standard deviation from both data sets.

The value of $\bar{s}(Rx'x, Rx"x)$ was calculated from the following equation:

$$\bar{s}(Rx'x, Rx"x) = \sqrt{\frac{\sum Rx'x + \sum Rx"x}{n_1+n_2-2}} \tag{6}$$

where: *Rx'x* i *Rx"x* – the value of the same roughness parameter referred to the simulation and experimental results, respectively.

The results of the analysis of the difference between two averages obtained by test *t* are presented in Table 4.

Table 4. The analysis of the difference between two averages obtained by test t applied to the roughness simulation and experimental test results (surface layer-workpiece)

Parameter	Calculated values of *t*	Critical values $t_{critical}$	
		$t_{0.05:6}$	$t_{0.1:6}$
Rz (μm)	0.65	2.447	1.943
Rp (μm)	0.37		
Rv (μm)	0.15		
RSm (μm)	1.83		

The comparison of the calculated values *t* with the critical values does not allow for the rejection of the zero hypotheses:

$$t < t_{0.05:6} \text{ and } t < t_{0.1:6} \tag{7}$$

Mapping geometrical structures of the steel roller's surface layer clear indicated on the pure micro-machining processes in the grinding operations (Fig. 14b). In our opinion this phenomenon is as a result of the very sharpen cutting edges and corners of the Cubitron II^{TM} abrasives grains, of the specifical grains orientation on the GWAS, of very big cutting depth and point contact between GWAS and the worpiece surface.

5. CONCLUSION

The results of model research and simulation and experimental tests allow us to draw the following conclusions:

- It is possible to build a simulation model of the process of the development of the geometrical structure of the surface layer of steel rollers machined with the Cubitron™ II grinding wheels by the Quickpoint technique. Such a possibility was demonstrated on the example of a correctly operating simulation model of the roughness development process between the surface layer and the workpiece,
- The correctness of the simulation model was positively influenced by the process of computer-aided recognition of the Cubitron™ II abrasive grains on the profile of the grinding-wheel circumference, as well as the assumption of a significant domination of the pure micro-machining processes in the grinding operations by the Quickpoint technique, especially in the conditions of increased grinding velocity (v_c = 50 m/s),
- For the grinding conditions specified in this paper, the values of the highest roughness profile *Rz*, the height of the largest peak of the profile *Rp*, the depth of the lowest valley of the profile *Rv*, and the average width of the grooves of the elements of the grinded surface profile, calculated in simulation tests, with the probability exceeding 90%, are equal to the values of the same roughness parameters determined in the experimental tests,

REFERENCES

[1] Catalog of Junker GmbH, 2011, *Quickpoint grinding*, 2011, Germany, www.junker-group.com Accessed 11 May 2017.
[2] KLOCKE F., BÜCKER C., 1996, *Quickpoint – Schleifen: Baustein einer flexiblen Produktion. Komplett bearbeiten in nur einer Aufspannung*, Ind. Anz, 118, 39-48.
[3] NIŻANKOWSKI CZ., 2013, *Technology and exploitation of grinding wheels made of sintered corundum used in surface grinding*, Politechnika Krakowska, Kraków, 135-146 (in Polish).
[4] Product Catalog of 3M, 2016, *Cubitron II – grinding wheels, Applied to life*, www.3m.pl/cubitron, 2-3 Accessed 30 July 2016.
[5] MARINESCU I.D., HITCHINER M. UHLMANN E., ROWE W.B., INASAKI I., 2011, *Handbook of machining with grinding wheels*, CRC Press, Boca Raton.
[6] JACKSON M.J. DAVIN J.P., 2011, *Machining with abrasives*, Springer, New York.
[7] JINYUAN H.C., WEIHUA T., CHEN Z.C., 2017, *The equal theoretical surface roughness grinding method for gear generating grinding*, The International Journal of Advanced Manufacturing Technology, 1-10, DOI: 10.1007/s00170-016-9651-8.

[8] KACALAK W., WOŹNIAK K., 1999, *Impact of grain shape on process and grinding results*, Postępy technologii maszyn I Urządzeń, z. 1 (in Polish).
[9] Product Catalogue of Polska Grupa Zbrojeniowa, 2016, International Defence Industry Exhibition MSPO, Kielce (in Polish).
[10] MARINESCU I.D., ROWE W.B., DIMITROV B., IMASAKI I., 2004, *Tribology of abrasive machining processes*. Wiliam Andrew Inc., Norwich.
[11] ADOLNY K., 2014, *State of the art in production, properties and applications of the microabrasive sintered corundum abrasive grains*, Int. J. Adv. Manuf. Technolog., 74/9, 1445-1449, doi: 10:1007/s00170-014-6090-2.
[12] WANG L.,TIAN X., LIU Q., LI Y., TANG X., YANG L., 2017, *Experimental study and theoretical analysis of the form grinding of gears using new type micro-crystal corundum grinding wheels*, The International Journal of Advanced Manufacturing Technology, 1–11, DOI: 10.1007/s00170-017-0246-9.
[13] WEBSTER J, TRICARD M., 2004, *Innovations in abrasive products for precision grinding*, CIRP Ann., 53/2, 590-610.
[14] CAO Y., BO J.G., XIAOLONG L., JIANGXINC., GAN J., 2013, *Modelling and simulation of grinding surface topography considering wheel vibration*, The International Journal of Advanced Manufacturing Technology, 66/5, 937-945.
[15] MAMALIS A.G., KUNDRÁK J., MANOLAKOS D.E., GYANI K., MARKOPOULOS A., HORVATH M., 2003, *Effect of the workpiece material on the heat affected zones during grinding: a numerical simulation*, The International Journal of Advanced Manufacturing Technology, 22/11, 761-767.
[16] WANG C., CHEN J., FANG Q., LIU F., LIU Y., 2016, *Study on brittle material removal in the grinding process utilizing theoretical analysis and numerical simulation*, The International Journal of Advanced Manufacturing Technology, 87/9, 2603-2614.
[17] YU H., WANG J., LU Y., 2016, *Simulation of grinding surface roughness using the grinding wheel with an abrasive phyllotactic pattern*, The International Journal of Advanced Manufacturing Technology, 84/5, 861-871.
[18] POLAŃSKI ZB., 1994, *Planning experience in technics*, PWN, 77-81, (in Polish).